Two Conserved Arginine Residues from the SK3 Potassium Channel Outer Vestibule Control Selectivity of Recognition by Scorpion Toxins*

Jing Feng[‡1], **Youtian Hu**[‡1], **Hong Yi**[‡1], **Shijin Yin**[‡], **Song Han**[‡], **Jun Hu**[‡], **Zongyun Chen**[‡], **Weishan Yang**[‡], **Zhijian Cao**[‡], **Michel De Waard**[§¶], **Jean-Marc Sabatier**[∥], **Wenxin Li**[‡], and **Yingliang Wu**[‡2]

From the ‡State Key Laboratory of Virology, College of Life Sciences, Wuhan University, Wuhan 430072, China, §INSERM U836, Grenoble Neuroscience Institute, Laboratory of Excellence, Ion Channels Science and Therapeutics, Université Joseph Fourier, 38042 Grenoble Cedex 09, France, ¶Smartox Biotechnology, 38700 La Tronche, France, and ∥INSERM UMR1097, Aix-Marseille Université, 13288 Marseille, France

Background: The SK channel mechanism that controls scorpion toxin recognition remains unknown.
Results: Two conserved arginine residues in the SK3 channel outer vestibule were found to control toxin recognition.
Conclusion: SK3 channel selectively controls toxin recognition through differential electrostatic repulsion forces between the channel vestibule and toxins.
Significance: These findings expand our understanding of the diverse channel structures and functions and unlock the pharmacological potential of toxins.

Potassium channel functions are often deciphered by using selective and potent scorpion toxins. Among these toxins, only a limited subset is capable of selectively blocking small conductance Ca^{2+}-activated K^+ (SK) channels. The structural bases of this selective SK channel recognition remain unclear. In this work, we demonstrate the key role of the electric charges of two conserved arginine residues (Arg-485 and Arg-489) from the SK3 channel outer vestibule in the selective recognition by the SK3-blocking BmP05 toxin. Indeed, individually substituting these residues with histidyl or lysyl (maintaining the positive electric charge partially or fully), although decreasing BmP05 affinity, still preserved the toxin sensitivity profile of the SK3 channel (as evidenced by the lack of recognition by many other types of potassium channel-sensitive charybdotoxin). In contrast, when Arg-485 or Arg-489 of the SK3 channel was mutated to an acidic (Glu) or alcoholic (Ser) amino acid residue, the channel lost its sensitivity to BmP05 and became susceptible to the "new" blocking activity by charybdotoxin. In addition to these SK3 channel basic residues important for sensitivity, two acidic residues, Asp-492 and Asp-518, also located in the SK3 channel outer vestibule, were identified as being critical for toxin affinity. Furthermore, molecular modeling data indicate the existence of a compact SK3 channel turret conformation (like a peptide screener), where the basic rings of Arg-485 and Arg-489 are stabilized by strong ionic interactions with Asp-492 and Asp-518. In conclusion, the unique properties of Arg-485 and Arg-489 (spatial orientations and

molecular interactions) in the SK3 channel account for its toxin sensitivity profile.

With ~100 members, the potassium channel family serves a variety of physiological functions and is involved in various channelopathies (1). Based on their activation mode and number of transmembrane segments, these channels can be classified according to four main structural types: (i) inwardly rectifying two-transmembrane K^+ channels (Kir), (ii) two-pore K^+ channels with four transmembrane segments (K2P), (iii) Ca^{2+}-activated K^+ channels with six or seven transmembrane segments (KCa), and (iv) voltage-gated K^+ channels with six transmembrane segments (Kv). Scorpion toxins are widely used to distinguish between these potassium channel types (2–4). Crystal structures of various potassium channels have recently been published, markedly increasing our knowledge of ion channel pores, selectivity filters, and gates (5–7). In two crystal structures of eukaryotic Kv1.2 and Kir2.2 channels, significant structural differences can be observed in the extracellular pore entryway, including turrets and filter regions, which are responsible for channel inactivation, toxin recognition, and interactions between channel subunits (Fig. 1). In contrast to the Kv1.2 extracellular pore entryway structure, the large turret and unusual TIGYGLR sequence in the filter region of Kir2.2 are responsible for its relative insensitivity to K^+ channel toxins (6, 7). In addition to these structural differences in the extracellular pore entryways between eukaryotic Kv1.2 and Kir2.2 channels, other specific structural differences have been identified by using scorpion toxins as molecular probes. In the human ERG (ether-à-go-go-related gene) channel (Fig. 1), also referred to as Kv11.1, unusually long turrets likely form a decentralized "petunia" shape, which could be probed by scorpion toxin BeKm-1 (8). Alternative models without a petunia shape are also proposed for the human ERG channel turret (9, 10). The conformation of the large conductance calcium-activated

---

[1] These authors contributed equally to this work.
[2] To whom correspondence should be addressed. Tel.: 86-27-6875-2831; Fax: 86-27-6875-6746; E-mail: ylwu@whu.edu.cn.

	Outer Helix	Turret		Pore Region	Inner Helix
SKCa3 :	LWIIA---WTVRVC RYH	--------------------DQQDVTS---N LG AMW LISITFL SIGYG DM VE H YCGK	---G VC LT
SKCa2 :	LWIIA---WTVRAC RYH	--------------------DQQDVTS---N LG AMW LISITFL SIGYG DM VE N YCGK	---G VC LT
SKCa1 :	SWIIA---WTVRVC RYH	--------------------DKQEVTS---N LG AMW LISITFL SIGYG DM VE H YCGK	---G VC LT
IKCa1 :	LWLTT---WVLSVA RQA	--------------------VNATG---HLSDT LW LIPITFL TIGYG DV VE G MWGK	---I VC CT
BK :	TAAGFI---HLVENSGDPWEN	------------------FQNNQAL---T WEC VY LLMVTMS TVGYG DY YAK U TLGR	---LFM VFF
KcsA :	YLAVL---------ERG	--------------------APGAQLI---T PR AL WSVETAT TVGYG DL YP V LWGR	---C VA VV
Kv1.2 :	SAVYF---------AD	--------------------ERESQFP---SIPD F WAVVSMT TVGYG DM TP V T IGGK	---I VGSLC
Kir2.2 :	WVIAV-----HGDL PAEGRGRT	----------------PCVMQVH---G MA FLFSIE TQT TIGYG LRCVTEECPV	---A F VV
hERG :	CI-WY---IGNMEQPHMDSRIGWLHNLGDQIGKPYNSSGLGGPSIKD	---K VT AL Y FTFSS LTS VGFG N VS N NSE	---IFS CV

FIGURE 1. **Sequence alignment of representative K⁺ channels.** The sequences represent the small conductance Ca²⁺-activated K⁺ channels (SK3, SK2, and SK1), the intermediate conductance Ca²⁺-activated K⁺ channels (IK), the large conductance Ca²⁺-activated K⁺ channel (BK), the potassium channel from *Streptomyces lividans* (KcsA), the voltage-gated potassium channel Kv1.2, the inwardly rectifying potassium channel Kir2.2, and the human ERG (*hERG*) potassium channel. Residues are *shaded* according to their degree of conservation. *Asterisks* indicate residues of the SK3 channel that were changed in later functional studies.

potassium (BK) channel turret varies from an open state conformation, for charybdotoxin (ChTX)[3] recognition, to a "helmet" conformation, for ChTX insensitivity, when the channel turret associates with the auxiliary β4 subunit (Fig. 1) (11). Overall, progress in characterizing extracellular pore entryways has demonstrated their significant structural and functional diversities. However, because of the present difficulty in solving crystal structures of additional eukaryotic potassium channels, further characterization of extracellular pore entryways of other potassium channels with unique functions remains a challenge.

Small conductance calcium-activated K⁺ (SK) channels are present predominantly in the nervous system (12, 13). They are involved in synaptic plasticity, fast glutamatergic synaptic potentials, and hippocampal learning (14–16). SK channels are efficiently blocked by several scorpion toxins, including BmP05, scyllatoxin, and P05, but are insensitive to many others (17, 18). Very few reports have investigated the structural features that underlie the specific recognition of SK channels by a restricted set of scorpion toxins. According to these studies, SK channel blockade would occur according to an "intermediate" mode of interaction (19) involving mainly the toxin α-helical structure rather than its β-sheet structure (20–22). Two arginyl residues found in an RRCQ motif present in both P05 and apamin are critical for P05 interaction with its target, as described for apamin (23). In contrast, the β-sheet structure appears to be important for a "pore-blocking" mode as far as Kv channel block is concerned (19, 24, 25). This distinctive mode of operation between SK channel-blocking and Kv channel-blocking toxins may be reconsidered taking into account the current state of knowledge of toxin interaction and computer-based simulation of toxin docking. Indeed, earlier studies were conducted based on less efficient docking simulations, and evidence is now increasing that the mode of toxin interaction with potassium channels may be switchable. In addition, channel turrets seem to play an important role in toxin docking. SK channel turret acidic residues were found to be involved in toxin binding in the intermediate mode (22, 26). Evidence has been provided that SK channel block by a maurotoxin-*Heterometrus spinifer* toxin-1 chimera is dependent on ionic strength (27, 28), suggesting that SK channel recognition by scorpion toxins involves some electrostatic charges. Acidic amino acid residues of toxins were found to affect the interac-

tion modes, further strengthening the importance of electrostatic interactions between toxins and channels (18). Herein, we explored the importance of electrostatic repulsion for the interaction of the α-helical structure of BmP05 with the SK3 channel. Introducing positively charged residues within the α-helical structure of BmP05 decreased toxin affinity. After identification of key positively charged residues of the SK3 channel turret (two conserved arginine residues at turret positions 485 and 489) and relevant mutations, we were able to render the SK3 channel sensitive to ChTX block by its β-sheet surface owing to its strong content of basic amino acid residues despite the fact that ChTX is pharmacologically unrelated to BmP05. Our data demonstrate that the mode of toxin/channel interaction can be altered by selective point mutations of the channel with the aid of appropriate computer-aided molecular simulations. We also show that the toxin sensitivity profile of SK3 channels is controlled by two conserved turret arginine residues that produce differential repulsive electrostatic forces with basic residues of scorpion toxins. These results further increase our understanding of the structural and functional diversity of potassium channel extracellular pore entryways and unlock the pharmacological potential of toxins.

EXPERIMENTAL PROCEDURES

Peptides and Potassium Channels—BmP05, its mutants, and ChTX were prepared according to a previously described procedure (29). The secondary structures of purified BmP05 and its mutants were measured by CD spectroscopy. Measurements were carried out in the UV range of 250–190 nm at 25 °C in water on a Jasco-810 spectropolarimeter with a 0.2–0.4 mg/ml concentration. For each peptide, spectra were collected from three separate recordings and averaged after subtracting the blank spectrum of pure water. The pEGFP-N1 plasmid containing the cDNAs for full-length human SK3 was kindly provided by Prof. Stephan Grissmer (University of Ulm, Ulm, Germany). Point mutations in SK3 were generated using the QuikChange mutagenesis kit (Stratagene) and subsequently confirmed by DNA sequencing (Invitrogen).

Cell Culture—HEK293 cells were cultured in Dulbecco's modified Eagle's medium (Invitrogen) supplemented with 10% fetal bovine serum and 1% penicillin/streptomycin in a humidified 5% CO₂ incubator at 37 °C. Cells were transfected using FuGENE transfection reagent (Roche Diagnostics) following

---

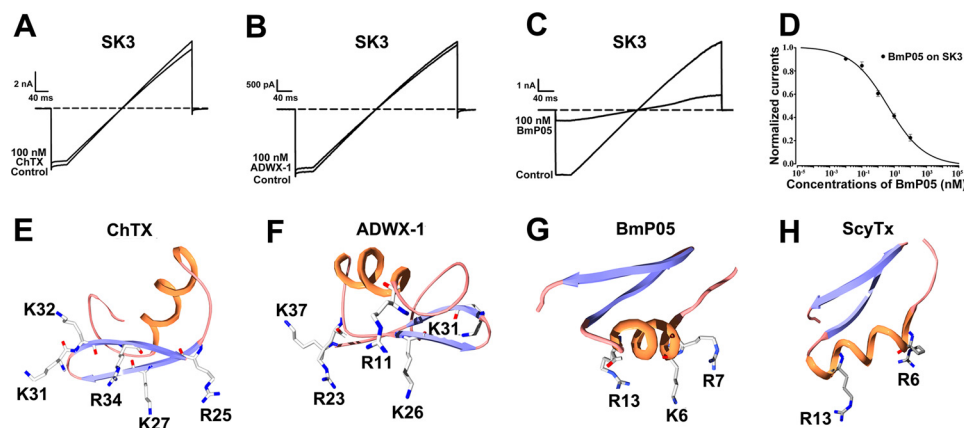[3] The abbreviation used is: ChTX, charybdotoxin.

FIGURE 2. **Selective recognition of SK3 channels by toxins with different channel-interacting surfaces.** *A–C*, inhibition of SK3 channel currents by 100 nm ChTX, ADWX-1, or BmP05 as indicated. BmP05 at 100 nm blocked ~80% of the SK3 currents (*C*), whereas ChTX and ADWX-1 were almost inactive (*A* and *B*). *D*, dose dependence of BmP05 block of SK3 currents. The fit of the curve provided an IC_{50} of 3.76 ± 1.24 nm. *E–H*, different channel-interacting surfaces: ChTX (Protein Data Bank code 2CRD), ADWX-1 (code 2K4U), BmP05, and scyllatoxin (*ScyTx*; code 1SCY). All toxin basic residues in their channel-binding surfaces are labeled.
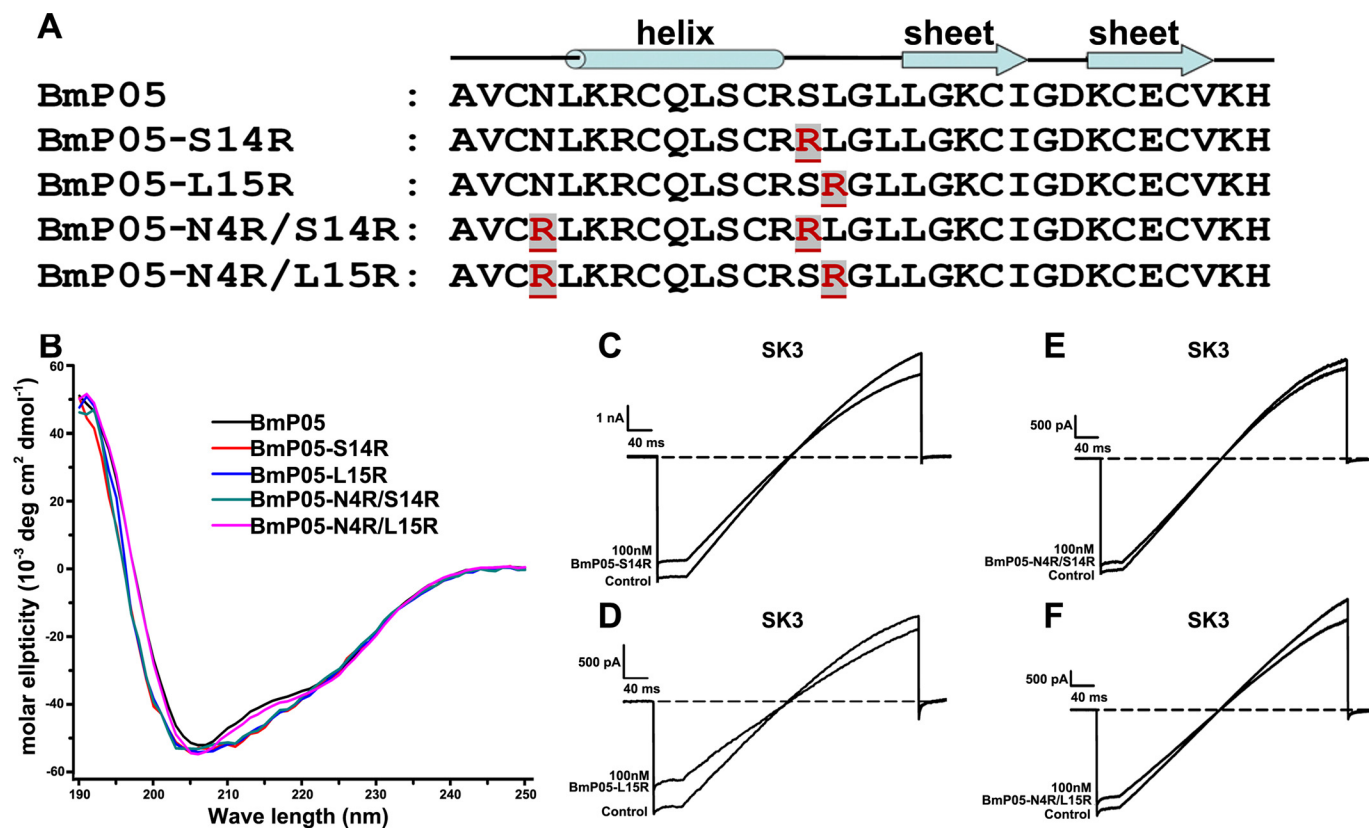

FIGURE 3. **Decreased BmP05 potency for SK3 channels resulting from increased content of basic residues in the BmP05 channel-binding surface.** *A*, one or two arginine residues (shown in *red*) were introduced into the channel-interacting surface. *B*, CD spectra of recombinant BmP05, BmP05-S14R, BmP05-L15R, BmP05-N4R/S14R, and BmP05-N4R/L15R peptides. Measurements were carried out in the UV range of 250–190 nm at 25 °C in water on a Jasco-810 spectropolarimeter at a concentration of 0.2–0.4 mg/ml. *C–F*, representative current traces of the SK3 channel showing reduced inhibition by 100 nm BmP05 mutants. *C*, 20.5% block by BmP05-S14R. *D*, 30.5% block by BmP05-L15R. *E*, 8.5% block by BmP05-N4R/S14R. *F*, 10.7% block by BmP05-N4R/L15R.

the manufacturer's instructions and used for electrophysiology 24–48 h after transfection.

Electrophysiology and Data Analyses—Electrophysiological experiments were performed at 22–25 °C using the patch clamp whole cell recording mode. For the recording, the bath contained 130 mm sodium aspartate, 30 mm potassium aspartate, 2 mm $CaCl_2$, 1 mm $MgCl_2$, and 10 mm HEPES (pH adjusted to 7.4 with NaOH). The pipette solution contained 145 mm potassium aspartate, 8.7 mm $CaCl_2$, 2 mm $MgCl_2$, 10 mm EGTA, and 10 mm HEPES (pH adjusted to 7.2 with KOH) to achieve an intracellular free Ca^{2+} concentration of 1 μM. The membrane potentials were clamped to −120 mV for 50 ms (which was used for the current measurements) followed by a 400-ms voltage ramp from −120 to +60 mV and were kept for 5 s between ramps at −40 mV using a HEKA EPC 10 amplifier with Patchmaster data acquisition software (HEKA Elektronik, Lam-
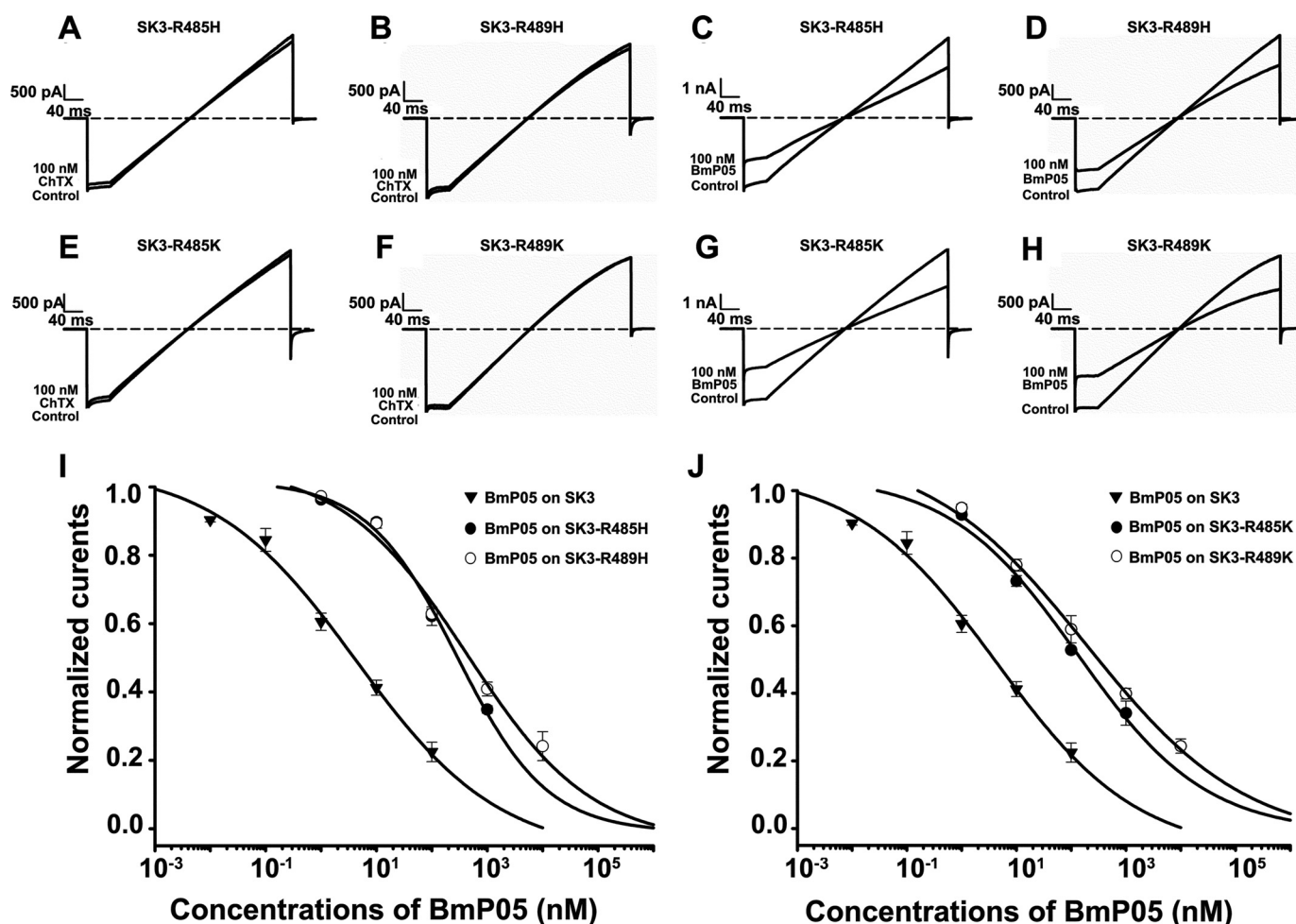
FIGURE 4. **Effects of substituting Arg-485 and Arg-489 with other basic residues on the SK3-blocking potency of BmP05.** *A–H*, representative current traces of SK3 channel mutants showing current blocks by BmP05 and ChTX. *A* and *B*, absence of inhibition of SK3-R485H and SK3-R489H currents by 100 nM ChTX. *C* and *D*, significant inhibition of SK3-R485H and SK3-R489H currents by 100 nM BmP05. *E* and *F*, lack of inhibition of SK3-R485K and SK3-R489K channels by 100 nM ChTX. *G* and *H*, significant inhibition of SK3-R485K and SK3-R489K channels by 100 nM BmP05. *I*, concentration dependence of SK3, SK3-R485H, and SK3-R489H current blocks by BmP05. The data were fitted and yielded IC_{50} values of 332.2 ± 84.9 nM (SK3-R485H) and 382.2 ± 141.1 nM (SK3-R489H). *J*, concentration dependence of SK3, SK3-R485K, and SK3-R489K current blocks by 100 nM BmP05. Fits of the data yielded IC_{50} values of 145.0 ± 55.1 nM (SK3-R485K) and 191.8 ± 60.5 nM (SK3-R489K). Data represent the means ± S.E. of at least three experiments.

brecht/Pfalz, Germany). All other chemicals were obtained from Sigma.

Data analyses were performed with IGOR software (WaveMetrics, Lake Oswego, OR). IC_{50} values were obtained by fitting a modified Hill equation to the data as shown in Equation 1,

$$I_{\text{toxin}}/I_{\text{control}} = 1/(1 + ([\text{toxin peptide}]/IC_{50}) \qquad \text{(Eq. 1)}$$

where I is the stable current at -120 mV for the normalized data points obtained with at least four different toxin peptide concentrations. Results are shown as the mean ± S.E. of at least three experiments.

Atomic Coordinates and Molecular Docking—The spatial structure of the pore region except for the turret of the SK3 channel was modeled using the crystallographic structure of the KcsA channel (Protein Data Bank code 1BL8) as a template with the SWISS-MODEL server (30). The turret of SK3 was built using the segment assembly homology modeling method as described previously (8, 11). An additional unrestrained molecular dynamics simulation was performed on

the model to obtain an equilibrated SK3 structure. The structure of BmP05 was modeled by using the atomic coordinates of the highly homologous scorpion toxin scyllatoxin (Protein Data Bank code 1SCY). BmP05 was docked onto the equilibrated SK3 structure using the ZDOCK program (31). Clustering analysis and experimental data-based screening were used to screen possible hits from the resulting complexes. These were then subjected to further molecular dynamics simulation to evaluate their stability and reasonability.

Molecular Dynamics Simulations—Molecular dynamics simulations were performed using the AMBER 11 program on the 128-CPU Dawning TC5000 cluster. The ff99 force field (parm99) (32) was applied throughout all of the simulation steps. Both the SK3 channel and BmP05-SK3 complex structures were subjected to unrestrained simulations in explicit solvent systems. The SK3 channel and the BmP05-SK3 complex were first embedded in a periodic box of 71.755 × 79.440 × 79.589 Å and 74.141 × 80.972 × 81.867 Å. A 5-ns pre-equilibration followed by a 10-ns unrestrained simulation was per-
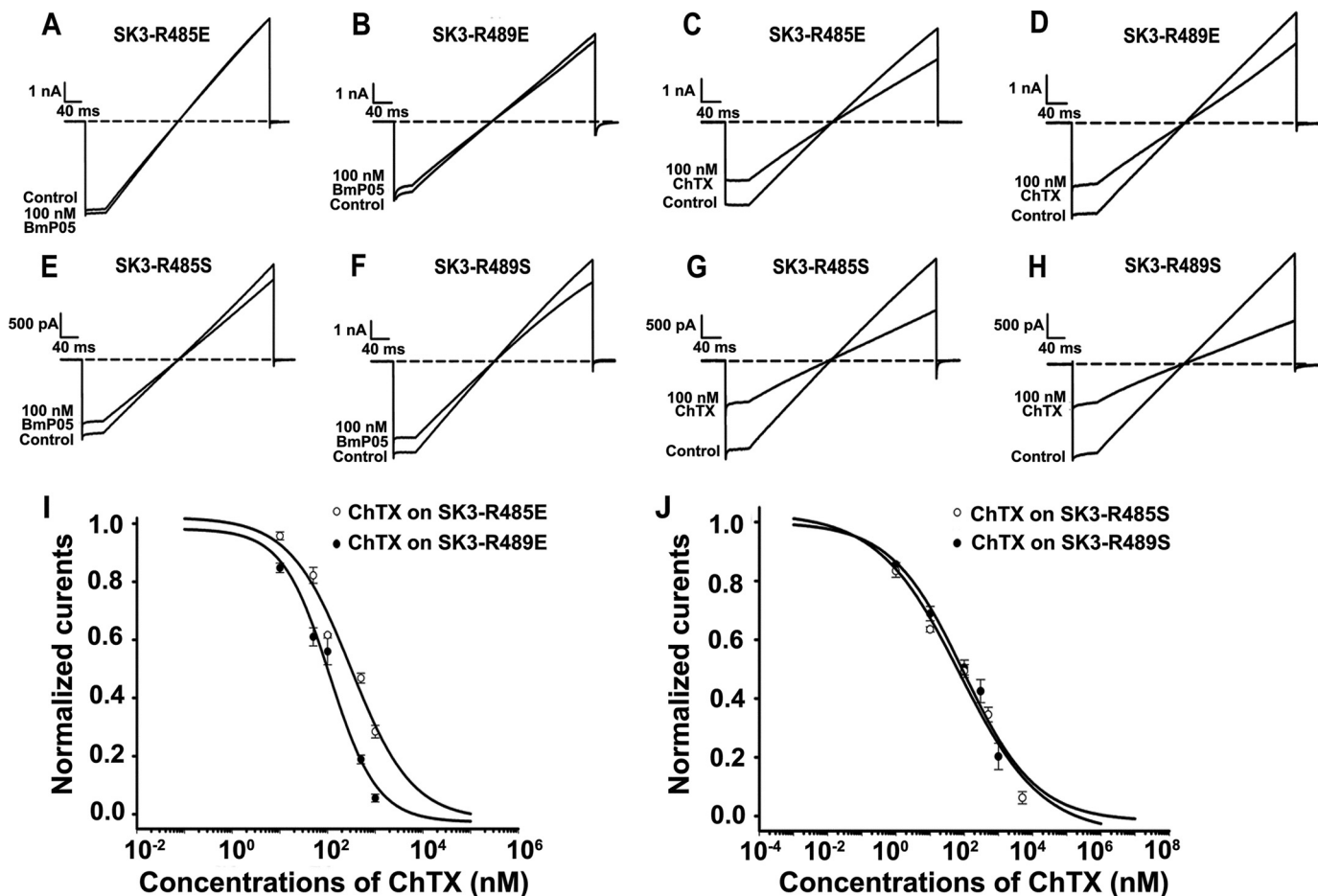
FIGURE 5. **Effects of substituting Arg-485 and Arg-489 with acidic or polar residues on the SK3-blocking potency of BmP05.** *A*–*H*, representative current traces of SK3 mutants showing current blocks by BmP05 and ChTX. *A* and *B*, reduced inhibition of SK3-R485E and SK3-R489E channels by 100 nM BmP05. *C* and *D*, significant inhibition of SK3-R485E and SK3-R489E currents by 100 nM ChTX. *E* and *F*, reduced inhibition of SK3-R485E and SK3-R489E channels by 100 nM BmP05. *G* and *H*, significant inhibition of SK3-R485S and SK3-R489S currents by 100 nM ChTX. *I*, concentration dependence of SK3-R485E and SK3-R489E current blocks by ChTX. Fits of the data yielded IC_{50} values of 381.7 ± 84.1 nM (SK3-R485E) and 110.7 ± 28.1 nM (SK3-R489E). *J*, concentration dependence of SK3-R485S and SK3-R489S current blocks by 100 nM ChTX. Fits of the data yielded IC_{50} values of 84.8 ± 21.6 nM (SK3-R485S) and 30.2 ± 4.5 nM (SK3-R489S). Data represent the mean ± S.E. of at least three experiments.

formed on the channel and the complex using the SANDER module in the AMBER 11 program to obtain sufficient stable conformations. The pre-equilibration steps were taken by gradually reducing the force constant from 5.0 kcal/mol/Å² for restraining all of the heavy atoms to 0.02 kcal/mol/Å² for backbone heavy atoms only. The temperature was set at 300 K with a cutoff distance of 10 Å.

RESULTS

The SK3 Channel Is Selectively Inhibited by Specific Scorpion Toxins Exhibiting No More than Three Basic Amino Acid Residues in Their Channel-binding Interfaces—As shown, the SK3 channels were almost insensitive to a 100 nM concentration of many types of the potassium channel-active ChTX toxin (Fig. 2*A*) or the Kv channel-active ADWX-1 peptide (Fig. 2*B*) (29). In contrast, 100 nM BmP05 inhibited ~80% of the SK3 channel current (Fig. 2*C*). The corresponding IC_{50} for of BmP05-induced current block is 3.8 nM (Fig. 2*D*). Structurally, there are four basic amino acid residues in the vicinity of the pore-blocking basic residue Lys-27 of ChTX or Lys-26 of ADWX-1 (Fig. 2, *E* and *F*). In contrast, the channel-binding

interface of BmP05 or scyllatoxin presents only three (Fig. 2*G*) or two (Fig. 2*H*) basic residues (33, 34). These structural differences in channel-binding interfaces suggest that the SK3 channel may be selectively recognized by scorpion toxins possessing three (or fewer) basic residues in these critical positions.

To further characterize the BmP05 channel-binding interface, we tested the effect of adding extra basic residue(s) on its ability to recognize the SK3 channel (Fig. 3*A*). Compared with the BmP05 peptide, the CD spectra of four mutants showed no significant changes in the secondary structure (Fig. 3*B*), indicating that BmP05 and its mutant peptides all adopted the same overall structural topology. Functionally, increasing the number of basic residues by one (at BmP05 position 14 or 15) or two (at BmP05 positions 4 and 14 or positions 4 and 15) arginyl residues strongly reduced its inhibitory potency at 100 nM on SK3 currents (Fig. 3, *C*–*F*). This decreased potency was stronger when two extra arginyl residues were incorporated into the BmP05 channel-binding interface (BmP05-N4R/S14R and BmP05-N4R/L15R) instead of a single residue (BmP05-S14R and BmP05-L15R) (Fig. 3, *E* and *F versus C* and *D*). From these
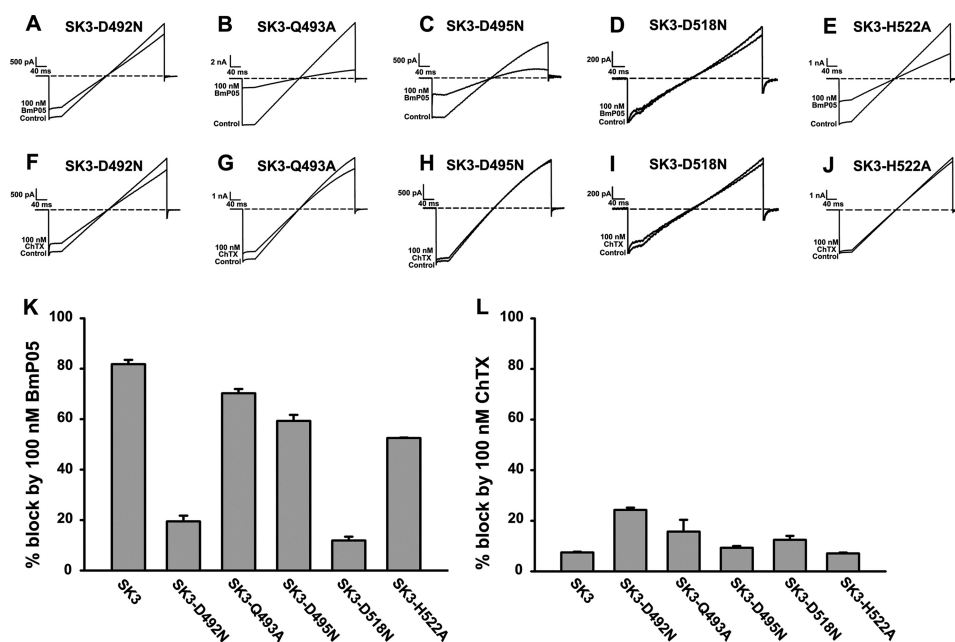
FIGURE 6. **Importance of other amino acid residues in the SK3 channel outer vestibule to potency of BmP05 and ChTX.** *A–J*, representative current traces of SK3 channel mutants showing current blocks by BmP05 and ChTX. *A* and *D*, reduced inhibition of SK3-D492N and SK3-D518N currents by 100 nM BmP05. *B*, *C*, and *E*, significant inhibition of SK3-Q493A, SK3-D495N, and SK3-H522A currents by 100 nM BmP05. *F–J*, decreased inhibition of SK3-D492N, SK3-Q493A, SK3-D495N, SK3-D518N, and SK3-H522A currents by 100 nM ChTX. *K*, average inhibition of wild-type and mutant SK3 channel currents by 100 nM BmP05. *L*, average inhibition of wild-type and mutant SK3 channel currents by 100 nM ChTX.

data, it appears that an efficient block of the SK3 channel by BmP05 occurs when three basic residues are located in the channel-binding interface of the toxin.

Substitution of the SK3 Channel Arg-485 or Arg-489 Basic Residue with Other Basic Residues Impairs BmP05 Affinity but Maintains the Differential BmP05/ChTX Sensitivity for the SK3 Channel—The sensitivity of BmP05 to the presence of extra basic amino acid residues in its binding interface strongly suggests the important role of electrostatic repulsion forces between the BmP05 channel-binding interface and the SK3 channel binding site. These electrostatic repulsion forces might occur with Arg-485 and Arg-489, two highly conserved basic residues that are located in the outer vestibules of all SK channel subtypes (Fig. 1). These electrostatic repulsion forces, if actually existing, can be diminished by replacing the wild-type Arg-485 or Arg-489 residue of the SK3 channel with less basic lysyl (SK3-R485K and SK3-R489K) or histidyl (SK3-R485H and SK3-R489H) residues. The resulting mutant channels were still insensitive to 100 nM ChTX (Fig. 4, *A*, *B*, *E*, and *F*) but maintained their sensitivity to 100 nM BmP05 (Fig. 4, *C*, *D*, *G*, and *H*), albeit at reduced levels. The degree of reduction in the BmP05 effect was assessed by dose-response analyses, and the results indicate affinity reductions of the mutant channels for BmP05 by 88-fold (SK3-R485H), 101-fold (SK3-R489H), 38-fold (SK3-R485K), and 51-fold (SK3-R489K) ($p < 0.05$) (Fig. 4, *I* and *J*). The reduction in affinity was higher for the Arg-to-His mutations, as expected from the less basic nature of the histidyl residue. The basic nature of the amino acid residues at SK3 positions 485 and 489 (*e.g.* Arg, Lys, or His) is key to maintaining the BmP05/ChTX selectivity for the SK3 channel, whereas the presence of arginyl residues at these positions is mandatory for maintaining high BmP05 affinity.

Replacement of Arg-485 and Arg-489 in the SK3 Channel with Acidic or Polar Residues Alters Its Relative Sensitivity to BmP05/ChTX—An additional step in weakening the electrostatic repulsion forces at the toxin/channel binding interface is to substitute the SK3 channel dyad of arginyl with acidic or polar amino acid residues. This was achieved by replacing Arg-485 or Arg-489 with a glutamic acid (acidic) or serine (polar) residue in the SK3 channel. In agreement with the importance of Arg-485 and Arg-489 in the high affinity of BmP05 for the SK3 channel, 100 nM BmP05 produced much less inhibition of the SK3-R485E (Fig. 5*A*), SK3-R489E (Fig. 5*B*), SK3-R485S (Fig. 5*E*), and SK3-R489S (Fig. 5*F*) mutant channels compared with the inhibition observed for the wild-type SK3 channel ($p < 0.05$) (Fig. 2, *C* and *D*). The electrically neutral serine residue was less prone to altering the electrostatic balance at the toxin/channel binding interface than the glutamic acid residue. This is consistent with the stronger current blocks of the SK3-R485S and SK3-R489S mutant channels by BmP05 compared with the current blocks of the SK3-R485E and SK3-R489E mutants. These data indicate that substitutions at positions 485 and 489 in the SK3 channel are sufficient to make the channel almost insensitive to BmP05, further strengthening the idea that these SK3 channel positions are key to toxin recognition. Interestingly, the potassium currents carried by all tested mutant channels were significantly blocked by 100 nM ChTX compared with wild-type SK3 channels ($p < 0.05$) (Figs. 2*A* and 5, *C*, *D*, *G*, and *H*). Dose-response analyses provided IC_{50} values for ChTX-induced current blocks of 381 nM (SK3-R485E), 110 nM (SK3-R489E), 84 nM (SK3-R485S), and 30 nM (SK3-R489S) (Fig. 5, *I* and *J*). These data are remarkable in the sense that a toxin, ChTX, known to block only Kv, BK, and intermediate conductance calcium-activated K^+ (IK) channels, can gain a novel
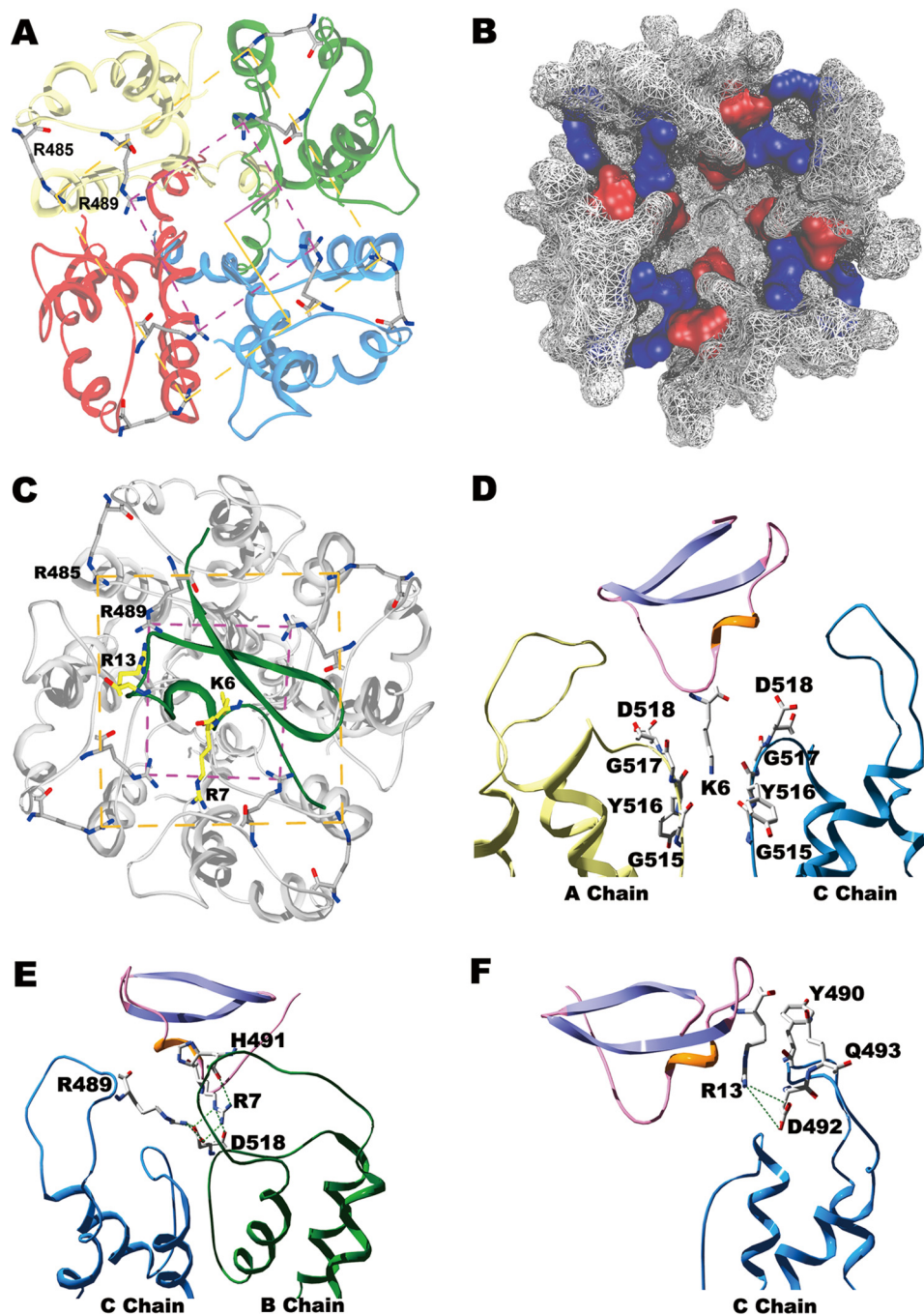
FIGURE 7. **Mechanism of selective SK3 channel recognition by scorpion toxins as addressed by molecular modeling and docking simulation approaches.** *A*, top view of the narrow gateway in the SK3 channel turrets. The large and small rings of basic residues are designated by *yellow* and *purple dashed lines*, respectively. *B*, molecular surface representation of the SK3 channel vestibule. Basic residues are shown in *blue*, and acidic residues are shown in *red*, as viewed from the extracellular side. *C*, interaction details of the BmP05-SK3 complex viewed from the extracellular side. To better distinguish between BmP05 and the SK3 channel, the toxin is colored *green*, and the SK3 channel in colored *gray*. *D*, Lys-6 of BmP05 plugged into the SK3 channel pore. The A and C chains are colored *yellow* and *cyan*, respectively. *E* and *F*, the functional residues within one SK3 channel turret that associate with Arg-7 and Arg-13 of BmP05 within a distance of 4 Å. The B and C chains are colored *green* and *cyan*, respectively.

activity for the SK3 channel if the latter is appropriately mutated at position 485 or 489. Furthermore, it is worth mentioning that, in this case, the appropriate mutations of the SK3 channel allow the channel to invert its pharmacological toxin sensitivity recognition profile from a BmP05-sensitive and ChTX-insensitive profile for the wild-type SK3 channel to a BmP05-insensitive and ChTX-sensitive profile for the appropriately mutated SK3 channel. Interestingly, these mutant SK3 channels acquire a pharmacological toxin sensitivity profile that resembles that of Kv channels, which are also BmP05-insensitive (18) and ChTX-sensitive.

Influence of Other Amino Acid Residues from the Outer Vestibule on the Relative SK3 Channel Sensitivity to BmP05/ChTX—Besides the dyad of arginyl residues (Arg-485 and Arg-489), we also investigated the effects of mutating other residues from the outer vestibule of the SK3 channel on its toxin sensitivity pro-
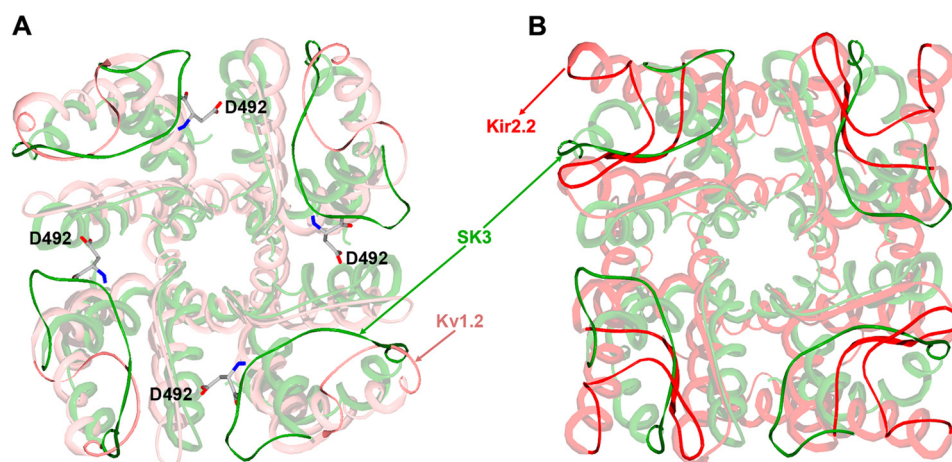
FIGURE 8. **More compact conformation of the SK3 channel turret.** *A*, superposition of the SK3 and rat Kv1.2 channels (Protein Data Bank code 2A79). *B*, superposition of the SK3 and rat Kir2.2 channels (code 3JYC). The SK3 channel is shown in *green*, the Kv1.2 channel is shown in *pink*, and the Kir2.2 channel is shown in *red*.

file. Many mutant SK3 channels were found to be inactive (SK3-E488A, SK3-E488N, SK3-Y490A, SK3-H491A, SK3-D492A, SK3-D495A, and SK3-D518A) and could not be investigated regarding this issue. However, five additional mutations (SK3-D492N, SK3-Q493A, SK3-D495N, SK3-D518N, and SK3-H522A) provided functional channels that could be characterized for their BmP05 and ChTX current blocks (Fig. 6, *A–E*). Two channels (SK3-D492N and SK3-D518N) were significantly less sensitive to BmP05 compared with wild-type SK3 channels ($p < 0.05$) (Fig. 6, *A*, *D*, and *K*), whereas three others (SK3-Q493A, SK3-D495N, and SK3-H522A) maintained an efficient BmP05 block compared with wild-type SK3 channels ($p < 0.05$) (Fig. 6, *B*, *C*, *E*, and *K*). Experimental IC_{50} values for the latter channel mutants were 16 nM (SK3-Q493A), 17 nM (SK3-D495N), and 82 nM (SK3-H522A) (data not shown). All SK3 channel mutants maintained the toxin sensitivity profile because none of the currents carried by these channels could be efficiently blocked by 100 nM ChTX ($p < 0.05$) (Fig. 6, *F–J* and *L*). These data clearly highlight the particular contribution of the arginyl dyad of the SK3 channel outer vestibule in defining its selective recognition by toxins.

DISCUSSION

Extracellular pore entryways are structurally important elements of potassium channels. They are involved in several functions, including channel inactivation, subunit interactions, and channel pharmacology. Due to the difficulties in solving potassium channel crystal structures (6, 7), potent scorpion toxins can be used to unravel potassium channel structure and function. In addition, significant conformational rearrangements in the toxin/channel recognition surfaces have been investigated and/or evidenced by computational simulation techniques (8, 11, 35) and by solid-state NMR spectroscopy (25, 36, 37). Herein, we investigated the SK3 channel structural determinants that are involved in the selective recognition by scorpion toxins by using BmP05 and ChTX as molecular probes. Our results point to the importance of a basic dyad, comprising the conserved Arg-485 and Arg-489 residues of the SK channel turret, as a critical structural determinant in defining the efficacy whereby the SK3 channel preferentially recognizes BmP05

over ChTX. Two questions deserve further attention. First, how does this dyad of SK3 residues impair the recognition of scorpion toxins such as ChTX? Second, how does the dyad influence the affinity/potency of SK3 channel-active toxins such as BmP05 for SK3 channels?

In an attempt to solve these questions, we modeled the structures of both the SK3 channel alone and the BmP05-SK3 complex using molecular modeling techniques (8, 11). As shown in Fig. 7 (*A* and *B*), the SK3 channel turret adopts a unique conformation in which both Arg-485 and Arg-489 form salt bridges with aspartic acid residues from adjacent SK3 subunits (Arg-485 with Asp-492; Arg-489 with both Asp-492 and Asp-518). These internal electrostatic interactions between the four channel turrets contribute to the formation of a narrow gateway together with the large ring (four Arg-485 residues) and small ring (four Arg-489 residues) of basic residues, as indicated by the structural superimposition of SK3 with the Kv1.2 and Kir2.2 structures (Fig. 8). These two rings of basic amino acid residues are conserved in the BmP05-SK3 complex structure (Fig. 7*C*). The unique structural properties (positions and interactions) of Arg-485 and Arg-489 (like a peptide screener) may account for the efficacy in governing scorpion toxin selectivity for the SK3 channel. As shown by the mutagenesis studies, the SK3 channel dyad of Arg-485 and Arg-489 is responsible for the toxin sensitivity of SK3 channels through differential electrostatic repulsion forces (Figs. 2 and 3). To minimize such forces, Lys-6 of BmP05 blocks the channel pore (Fig. 7, *C* and *D*), similar to Lys-27 of ChTX or Lys-26 of ADWX-1 (11, 29). Arg-7 of BmP05 is located between two Arg-489 residues that form the small ring of basic residues, whereas Arg-13 of the toxin hangs just above the two rings of Arg-485 and Arg-489 (Fig. 7*C*). Obviously, toxins with a greater number of basic amino acid residues in the channel-interacting surface are unable to recognize the SK3 channel owing to stronger electrostatic repulsion forces between the toxin and basic rings of the arginine residues (as evidenced in Figs. 2 and 3). The toxin recognition profile of SK3 channels (sensitive to BmP05 and insensitive to ChTX) is maintained by basic amino acid substitutions of the arginyl dyad (Fig. 4) but inverted by acidic or polar amino acid residue

replacements (Fig. 5). At the structural level, these results can be interpreted by the maintenance or disappearance of basic rings depending on the nature of residue substitutions, *i.e.* preserved if the dyad is mutated to basic amino acid residues and lost if acidic or polar residues are selected instead. In this respect, it is interesting to note that the loss of one of the two basic rings "drives" an SK3 channel toward a BK-type channel by rendering the modified SK3 channel insensitive to BmP05 (18) and sensitive to ChTX. The functional and modeling data point to an exquisite role of the two conserved Arg-485 and Arg-489 residues as being essential determinants of the SK3 channel with regard to its recognition profile of toxins.

It is worth emphasizing that the two conserved Arg-485 and Arg-489 residues of the SK3 channel are also essential for the potency of SK3-blocking toxins by maintaining the unique narrow gateway conformation of the channel turrets (Fig. 7, *A* and *B*), which are critical domains for scorpion toxin interactions (Fig. 7, *E* and *F*). The BmP05 affinity for the SK3 channel decreases significantly when these arginyl residues are replaced with less basic ones (Fig. 4). This may result in a looser conformation of the channel turrets as a consequence of weaker electrostatic interactions between the four SK3 channel subunits (Fig. 7, *A* and *B*). The looser turret structure presumably impairs the interactions of BmP05 Arg-7 and Arg-13 with the critical residues from the SK3 channel turrets (Fig. 7, *E* and *F*). The D492N or D518N mutation, conferring BmP05 insensitivity to modified SK3 channels (Fig. 6), also disrupts some key electrostatic interactions between channel subunits, thereby conferring looser turret structures (Fig. 7, *A* and *B*). These data strongly suggest that the potency of SK3-blocking scorpion toxins is dependent on the narrow gateway structure of the SK3 outer vestibule, itself constrained by the electrostatic interactions of Arg-485 and Arg-489 with acidic residues.

In conclusion, this work describes the unique properties of two conserved SK3 channel Arg-485 and Arg-489 residues in controlling selective scorpion toxin recognition. Our findings contribute to a better understanding of the molecular mechanisms involved in the selective recognition of SK channels by scorpion toxins. Undoubtedly, they provide structural and mechanistic insights for the design of selective peptide inhibitors specific to each subtype of SK channel. Indeed, subtype-specific SK channel blockers would be useful to treat neurological disorders more effectively (38).

REFERENCES

1. Ashcroft, F. M. (2006) From molecule to malady. *Nature* **440,** 440–447
2. Gross, A., and MacKinnon, R. (1996) Agitoxin footprinting the *Shaker* potassium channel pore. *Neuron* **16,** 399–406
3. MacKinnon, R., Cohen, S. L., Kuo, A., Lee, A., and Chait, B. T. (1998) Structural conservation in prokaryotic and eukaryotic potassium channels. *Science* **280,** 106–109
4. Lu, Z., Klem, A. M., and Ramu, Y. (2001) Ion conduction pore is conserved among potassium channels. *Nature* **413,** 809–813
5. Doyle, D. A., Morais Cabral, J., Pfuetzner, R. A., Kuo, A., Gulbis, J. M., Cohen, S. L., Chait, B. T., and MacKinnon, R. (1998) The structure of the potassium channel: molecular basis of K$^+$ conduction and selectivity. *Science* **280,** 69–77
6. Long, S. B., Campbell, E. B., and Mackinnon, R. (2005) Crystal structure of a mammalian voltage-dependent *Shaker* family K$^+$ channel. *Science* **309,** 897–903
7. Tao, X., Avalos, J. L., Chen, J., and MacKinnon, R. (2009) Crystal structure of the eukaryotic strong inward-rectifier K$^+$ channel Kir2.2 at 3.1 Å resolution. *Science* **326,** 1668–1674
8. Yi, H., Cao, Z., Yin, S., Dai, C., Wu, Y., and Li, W. (2007) Interaction simulation of hERG K$^+$ channel with its specific BeKm-1 peptide: insights into the selectivity of molecular recognition. *J. Proteome Res.* **6,** 611–620
9. Subbotina, J., Yarov-Yarovoy, V., Lees-Miller, J., Durdagi, S., Guo, J., Duff, H. J., and Noskov, S. Y. (2010) Structural refinement of the hERG1 pore and voltage-sensing domains with ROSETTA-membrane and molecular dynamics simulations. *Proteins* **78,** 2922–2934
10. Tseng, G. N., Sonawane, K. D., Korolkova, Y. V., Zhang, M., Liu, J., Grishin, E. V., and Guy, H. R. (2007) Probing the outer mouth structure of the HERG channel with peptide toxin footprinting and molecular modeling. *Biophys. J.* **92,** 3524–3540
11. Gan, G., Yi, H., Chen, M., Sun, L., Li, W., Wu, Y., and Ding, J. (2008) Structural basis for toxin resistance of β4-associated calcium-activated potassium (BK) channels. *J. Biol. Chem.* **283,** 24177–24184
12. Stocker, M. (2004) Ca^{2+}-activated K$^+$ channels: molecular determinants and function of the SK family. *Nat. Rev. Neurosci.* **5,** 758–770
13. Berkefeld, H., Fakler, B., and Schulte, U. (2010) Ca^{2+}-activated K$^+$ channels: from protein complexes to function. *Physiol. Rev.* **90,** 1437–1459
14. Stackman, R. W., Hammond, R. S., Linardatos, E., Gerlach, A., Maylie, J., Adelman, J. P., and Tzounopoulos, T. (2002) Small conductance Ca^{2+}-activated K$^+$ channels modulate synaptic plasticity and memory encoding. *J. Neurosci.* **22,** 10163–10171
15. Hammond, R. S., Bond, C. T., Strassmaier, T., Ngo-Anh, T. J., Adelman, J. P., Maylie, J., and Stackman, R. W. (2006) Small-conductance Ca^{2+}-activated K$^+$ channel type 2 (SK2) modulates hippocampal learning, memory, and synaptic plasticity. *J. Neurosci.* **26,** 1844–1853
16. Faber, E. S., Delaney, A. J., and Sah, P. (2005) SK channels regulate excitatory synaptic transmission and plasticity in the lateral amygdala. *Nat. Neurosci.* **8,** 635–641
17. Rodríguez de la Vega, R. C., and Possani, L. D. (2004) Current views on scorpion toxins specific for K$^+$-channels. *Toxicon* **43,** 865–875
18. Han, S., Yin, S., Yi, H., Mouhat, S., Qiu, S., Cao, Z., Sabatier, J. M., Wu, Y., and Li, W. (2010) Protein-protein recognition control by modulating electrostatic interactions. *J. Proteome Res.* **9,** 3118–3125
19. Rodríguez de la Vega, R. C., Merino, E., Becerril, B., and Possani, L. D. (2003) Novel interactions between K$^+$ channels and scorpion toxins. *Trends Pharmacol. Sci.* **24,** 222–227
20. Cui, M., Shen, J., Briggs, J. M., Fu, W., Wu, J., Zhang, Y., Luo, X., Chi, Z., Ji, R., Jiang, H., and Chen, K. (2002) Brownian dynamics simulations of the recognition of the scorpion toxin P05 with the small-conductance calcium-activated potassium channels. *J. Mol. Biol.* **318,** 417–428
21. Regaya, I., Beeton, C., Ferrat, G., Andreotti, N., Darbon, H., De Waard, M., and Sabatier, J. M. (2004) Evidence for domain-specific recognition of SK and Kv channels by MTX and HsTx1 scorpion toxins. *J. Biol. Chem.* **279,** 55690–55696
22. Andreotti, N., di Luccio, E., Sampieri, F., De Waard, M., and Sabatier, J. M. (2005) Molecular modeling and docking simulations of scorpion toxins and related analogs on human SKCa2 and SKCa3 channels. *Peptides* **26,** 1095–1108
23. Sabatier, J. M., Zerrouk, H., Darbon, H., Mabrouk, K., Benslimane, A., Rochat, H., Martin-Eauclaire, M. F., and Van Rietschoten, J. (1993) P05, a new leiurotoxin I-like scorpion toxin: synthesis and structure-activity relationships of the α-amidated analog, a ligand of Ca^{2+}-activated K$^+$ channels with increased affinity. *Biochemistry* **32,** 2763–2770
24. Yu, L., Sun, C., Song, D., Shen, J., Xu, N., Gunasekera, A., Hajduk, P. J., and Olejniczak, E. T. (2005) Nuclear magnetic resonance structural studies of a potassium channel-charybdotoxin complex. *Biochemistry* **44,** 15834–15841
25. Lange, A., Giller, K., Hornig, S., Martin-Eauclaire, M. F., Pongs, O., Becker, S., and Baldus, M. (2006) Toxin-induced conformational changes in a

potassium channel revealed by solid-state NMR. *Nature* **440,** 959 –962

26. Wittekindt, O. H., Visan, V., Tomita, H., Imtiaz, F., Gargus, J. J., Lehmann-Horn, F., Grissmer, S., and Morris-Rosendahl, D. J. (2004) An apamin- and scyllatoxin-insensitive isoform of the human SK3 channel. *Mol. Pharmacol.* **65,** 788 – 801

27. Shakkottai, V. G., Regaya, I., Wulff, H., Fajloun, Z., Tomita, H., Fathallah, M., Cahalan, M. D., Gargus, J. J., Sabatier, J. M., and Chandy, K. G. (2001) Design and characterization of a highly selective peptide inhibitor of the small conductance calcium-activated K$^+$ channel, SkCa2. *J. Biol. Chem.* **276,** 43145– 43151

28. Castle, N. A., London, D. O., Creech, C., Fajloun, Z., Stocker, J. W., and Sabatier, J. M. (2003) Maurotoxin: a potent inhibitor of intermediate conductance Ca^{2+}-activated potassium channels. *Mol. Pharmacol.* **63,** 409 – 418

29. Han, S., Yi, H., Yin, S. J., Chen, Z. Y., Liu, H., Cao, Z. J., Wu, Y. L., and Li, W. X. (2008) Structural basis of a potent peptide inhibitor designed for Kv1.3 channel, a therapeutic target of autoimmune disease. *J. Biol. Chem.* **283,** 19058 –19065

30. Guex, N., and Peitsch, M. C. (1997) SWISS-MODEL and the Swiss-Pdb-Viewer: an environment for comparative protein modeling. *Electrophoresis* **18,** 2714 –2723

31. Chen, R., Li, L., and Weng, Z. (2003) ZDOCK: an initial-stage protein-docking algorithm. *Proteins* **52,** 80 – 87

32. Wang, J., Cieplak, P., and Kollman, P. A. (2000) How well does a restrained electrostatic potential (RESP) model perform in calculating conformational energies of organic and biological molecules? *J. Comput. Chem.* **21,** 1049 –1074

33. Wu, J. J., He, L. L., Zhou, Z., and Chi, C. W. (2002) Gene expression, mutation, and structure-function relationship of scorpion toxin BmP05 active on SK$_{Ca}$ channels. *Biochemistry* **41,** 2844 –2849

34. Pease, J. H., and Wemmer, D. E. (1988) Solution structure of apamin determined by nuclear magnetic resonance and distance geometry. *Biochemistry* **27,** 8491– 8498

35. Yin, S. J., Jiang, L., Yi, H., Han, S., Yang, D. W., Liu, M. L., Liu, H., Cao, Z. J., Wu, Y. L., and Li, W. X. (2008) Different residues in channel turret determining the selectivity of ADWX-1 inhibitor peptide between Kv1.1 and Kv1.3 channels. *J. Proteome Res.* **7,** 4890 – 4897

36. Ader, C., Schneider, R., Hornig, S., Velisetty, P., Wilson, E. M., Lange, A., Giller, K., Ohmert, I., Martin-Eauclaire, M. F., Trauner, D., Becker, S., Pongs, O., and Baldus, M. (2008) A structural link between inactivation and block of a K$^+$ channel. *Nat. Struct. Mol. Biol.* **15,** 605– 612

37. Ader, C., Schneider, R., Hornig, S., Velisetty, P., Vardanyan, V., Giller, K., Ohmert, I., Becker, S., Pongs, O., and Baldus, M. (2009) Coupling of activation and inactivation gate in a K$^+$-channel: potassium and ligand sensitivity. *EMBO J.* **28,** 2825–2834

38. Wulff, H., and Zhorov, B. S. (2008) K$^+$ channel modulators for the treatment of neurological disorders and autoimmune diseases. *Chem. Rev.* **108,** 1744 –1773